

Heterogeneity in two-dimensional melting

HAYATO SHIBA, TAKEAKI ARAKI and AKIRA ONUKI

Department of Physics, Kyoto University, Kyoto 606-8502, Japan

PACS 64.70.D- – Solid-liquid transitions
 PACS 61.4.-j – Disordered solids
 PACS 83.10.Rs – Computer simulation of molecular and particle dynamics

Abstract. - Using molecular dynamics simulation we study structural and dynamic heterogeneity at the melting in one and two component systems in two dimensions. We define a disorder variable D_j for each particle j , which measures the degree of deviations from the hexagonal order. Between solid and liquid we find intermediate states, which are characterized by coexistence of crystalline and liquid-like disordered regions on mesoscopic scales in a temperature window. The changeovers among these three phases are continuous. We find that the structure factors of the density and the composition are considerably enhanced at long wavelengths in the intermediate phase.

Introduction. – Since a pioneering simulation by Alder and Wainwright [1], much attention has been paid to the two dimensional (2D) melting in simple one component particle systems [2, 3]. However, it has been controversial whether the transition is first order as in three dimensional melting [1, 4–6] or is continuous as predicted by Halperin and Nelson [7] and by Young [8]. The latter authors presented a defect-mediated melting mechanism and a "hexatic phase" in a temperature (or density) window between crystal and liquid. In this intermediate phase, the bond-orientation correlation function $g_6(r)$ of a sixfold orientation order parameter $\psi_6(\mathbf{r})$ decays algebraically, but the density correlation function $g(r)$ decays exponentially. That is, there is a long-range orientational correlation without long-range positional order in the hexatic phase. These predictions have been confirmed in experiments [9–16] and simulations [17–19]. In more detail, defects have been observed to proliferate and form grain boundaries with increasing the temperature T or the density n [12, 20, 21]. As other theories, Chui proposed another melting mechanism mediated by grain boundaries [22], while Saito argued that the 2D melting can be either continuous or first order depending on the specific details of the system [23].

As a marked feature, a number of experiments and simulations have been observing heterogeneity in the hexagonal structures [9, 10, 12, 15, 21, 24] and in the particle trajectories [1, 11, 16, 21, 25], developing around the transition on mesoscopic spatial scales. In particular, strong dependence on the system size has been encountered in the cal-

culations of the equation of state (in the plane of the pressure p and the density n) [1, 6, 17, 19] and of the local fluctuations of $\psi_6(\mathbf{r})$ in a finite-size scaling analysis [6]. We may ascribe the origin of such size-dependence to appearance of mesoscopic ordered and disordered regions (or clusters) as in critical phenomena. However, the heterogeneity in the 2D melting has not yet been well understood despite numerous papers in the field. The aim of this Letter is hence to visualize the heterogeneity unambiguously using a disorder variable introduced recently [21] and study its origin in more detail.

There have also been investigations of the 2D melting in binary mixtures of large and small particles with size ratio $\sigma_2/\sigma_1 > 1$, where σ_1 and σ_2 are the diameters of the particles [26–28]. It is highly nontrivial how the melting transition is altered with such size dispersity. If σ_2/σ_1 is close to 1, crystalline states with a small number of defects are realized. If it deviates considerably from 1 (say, at 1.3), glassy states follow for not small concentration c of the large particles, as has been studied extensively [3, 29–31]. Furthermore, polycrystal intervenes between crystal and glass at low T in a rather narrow region of σ_2/σ_1 and c , where the grain boundaries are pinned [21, 32]. In this Letter, we will also examine the melting of a polycrystal state, where intermediate states are still realized for small c between solid and liquid. We shall see that comparison between the one and two component cases is informative on the heterogeneity mechanism.

Theoretical Background. – In 2D dense particle systems, a large fraction of the particles are enclosed by six

particles and the local order is represented by the sixfold orientation [7]. We define the orientation angle α_j in the range $[-\pi/6, \pi/6]$ for each particle j using the complex number

$$\Psi_j = \sum_{k \in \text{bonded}} \exp[6i\theta_{jk}] = |\Psi_j| e^{6i\alpha_j}. \quad (1)$$

where the distance $|\mathbf{r}_j - \mathbf{r}_k|$ between the particles j and k is shorter than $1.25\sigma_{\alpha\beta}$ [21, 29]. Next we construct another nonnegative-definite variable representing the degree of disorder for each particle j by [21]

$$D_j = 2 \sum_{k \in \text{bonded}} [1 - \cos 6(\alpha_j - \alpha_k)]. \quad (2)$$

The D_j is nearly zero for a perfect crystal, but is large in the range 5 – 20 for particles around defects. Thus D_j is convenient in visualizing the structural inhomogeneity.

In terms of the angles α_j the sixfold orientation order parameter $\psi_6(\mathbf{r})$ is defined as [7, 8]

$$\psi_6(\mathbf{r}) \equiv \sum_{j=1}^N e^{6i\alpha_j} \delta(\mathbf{r} - \mathbf{r}_j). \quad (3)$$

In the hexatic phase, the bond-orientational correlation function decays as

$$g_6(r) = \langle \psi_6(\mathbf{r}) \psi_6(\mathbf{0})^* \rangle \sim r^{-\eta}, \quad (4)$$

where $r = |\mathbf{r}|$ and the exponent η is dependent on the temperature T and the density n .

Numerical Method. – Our 2D system is composed of $N = N_1 + N_2 = 9000$ particles interacting via a truncated Lennard-Jones potential of the form

$$v_{\alpha\beta}(r) = 4\epsilon [(\sigma_{\alpha\beta}/r)^{12} - (\sigma_{\alpha\beta}/r)^6] - C_{\alpha\beta}, \quad (5)$$

where $\alpha, \beta = 1, 2$. This potential is characterized by the energy ϵ and the range $\sigma_{\alpha\beta} = (\sigma_\alpha + \sigma_\beta)/2$. For $r > r_{\text{cut}} = 3.2\sigma_1$, we set $v_{\alpha\beta}(r) = 0$ and the constant $C_{\alpha\beta}$ ensures the continuity of $v_{\alpha\beta}(r)$ at the cut-off $r = r_{\text{cut}}$. The one component case is obtained for $\sigma_2/\sigma_1 = 1$. The mixture case is realized for $\sigma_2/\sigma_1 > 1$, where the large particles constitute the second component. The system volume V is fixed such that the areal fraction of the soft-core regions is fixed at 0.9 or at $\phi = (N_1\sigma_1^2 + N_2\sigma_2^2)/V = 0.9$. We integrated the equations of motion using the Störmer-Verlet algorithm (a sort of the leap-frog method) under the periodic boundary conditions using the Nosé-Hoover thermostat. The time step of integration is 0.002τ with

$$\tau = \sigma_1 \sqrt{m_1/\epsilon}. \quad (6)$$

In our simulations, we first quenched the system from $T = 2\epsilon/k_B$ to $0.2\epsilon/k_B$ into a crystal or polycrystal state. After a relaxation time of $5 \times 10^3\tau$, there was no appreciable time evolution of the physical quantities such as the pressure [21]. We then increased T to a desired value. The time t is set equal to 0 at this increase. Hereafter we will measure space, time, and T in units of σ_1 , τ , and ϵ/k_B , respectively.

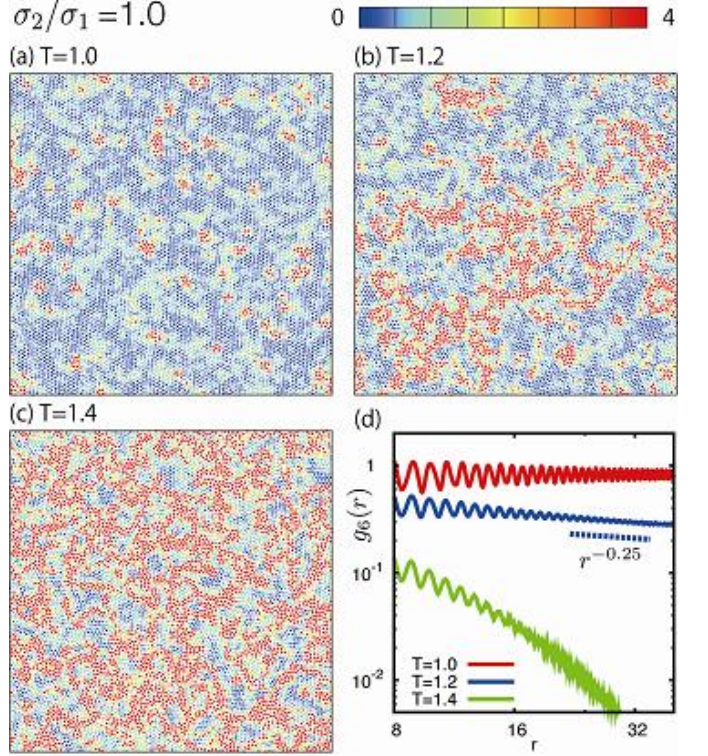


Fig. 1: Disorder variable D_j in a one component system at $t = 10^4$ for (a) $T = 1.0$ (solid), (b) $T = 1.2$ (hexatic), and (c) 1.4 (liquid). The color is given according to the color bar (top). It is red for the particles with $D_i > 4$. Shown also is the bond-orientation correlation function $g_6(r)$ for (a)-(c).

Structural Heterogeneity. – In fig. 1, we display all the particles with D_j in a one component system for $T = 1.0, 1.2$, and 1.4 at $t = 10^4$. The average disorder parameter $\bar{D} = \sum_i D_i/N$ over the particles is 1.10, 2.54, and 3.84 for these cases. They are snapshots in a solid, hexatic, and liquid state, respectively, as can be known from the decay of the bond-orientational correlation function $g_6(r)$. In fig. 1, it decays as $r^{-\eta}$ with $\eta = 0.27$ for (b) and exponentially for (c), while there is no decay for (a). Theoretically [7, 8], η tends to $1/4$ as the system approaches the transition to liquid. We can see that defects form grain boundaries in (b) as in the previous observations [12, 20, 21]. We may regard the particles with $D_j > 4$ (red in the figures) as “disordered”. In the crystal state (a) at $T = 1.0$ they are localized around dislocations. In the hexatic state (b) at $T = 1.2$ they appear collectively to form mesoscopic disordered regions (or clusters), which closely resemble the critical fluctuations in spin systems [33]. These heterogeneous structures emerge, move, and decay on a time scale of order 10τ as thermal fluctuations. In the liquid state (c) at $T = 1.4$ a majority of the particles are disordered.

In fig. 2, snapshots of D_j are shown in a binary mixture with $\sigma_2/\sigma_1 = 1.4$ and $c = N_2/N = 0.05$ for $T = 0.2, 0.6, 0.8$, and 1.0 . The corresponding value of $\bar{D} = \sum_i D_i/N$ is

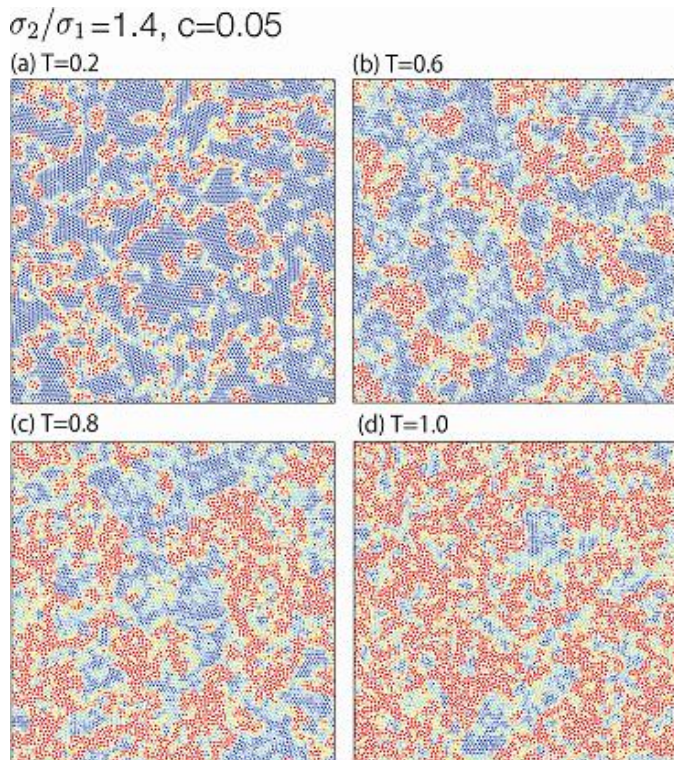


Fig. 2: Disorder variable D_j in a binary mixture at $t = 10^4$ with $\sigma_2/\sigma_1 = 1.4$ and $c = 0.05$, where (a) $T = 0.2$ (polycrystal), (b) $T = 0.6$ (intermediate), (c) $T = 0.8$ (intermediate), and (d) $T = 1.0$ (liquid). The large particles are in the disordered regions. The color is given as in fig. 1.

1.67, 2.19, 3.05, and 4.02, respectively. In these states, the large particles are surrounded by small particles with high D_j . In (a) at $T = 0.2$ a polycrystal state is realized, where the grain boundaries are formed around the large particles and are pinned or immobile. For this size ratio, the crystalline regions consist of the small particles only [34]. The typical grain size is of order $10\sigma_1$ (but it decreases with increasing c , eventually resulting in glass [32]). In (b) at $T = 0.6$ the grain boundaries are thickened and broken, resulting in disordered regions containing the large particles. In (c) at $T = 0.8$ the disordered regions are further increased. In (d) at $T = 1.0$ a liquid state is reached. In addition, in fig. 3, we show the positions of the large particles in the intermediate states (b) and (c) in fig. 2. They tend to aggregate in narrower regions in (b) than in (c).

The correlation function $g_6(r)$ in the mixture case is apparently more short-ranged than in the one component case even for $c \ll 1$. That is, in the intermediate states (b) and (c), there is a crossover length $\ell(c)$ determined by c and $g_6(r)$ decays exponentially for $r > \ell(c)$. In the polycrystal state (a), $g_6(r)$ decays on the scale of the grain size. In the liquid state (d), $g(r)$ decays exponentially with a microscopic correlation length. However, we have not yet obtained reliable data of $g_6(r)$ in the polycrystal and intermediate states because of the very slow time evolution

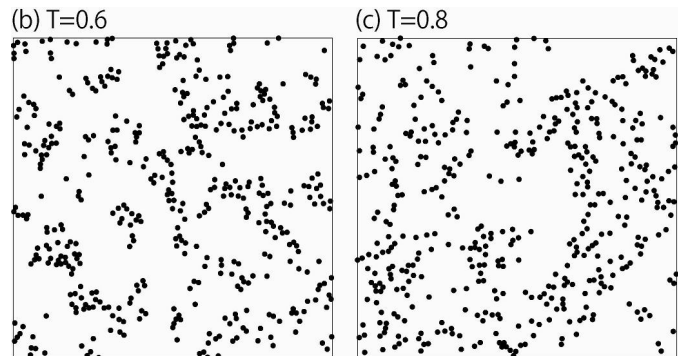


Fig. 3: 450 large particles in the intermediate states, (b) at $T = 0.6$ and (c) at $T = 0.8$, in fig. 2. Their distribution exhibits large-scale heterogeneity. See the corresponding structure factors in fig. 6.

in the the present system size.

In fig. 4, we show the fraction ϕ_D of the disordered particles with $D_j > 4$. It is defined by $\phi_D = N_D/N$, where N_D is the number of the disordered particles. For the one component case, it nearly vanishes in solid and abruptly increases in the hexatic phase. For the mixture case with $\sigma_1/\sigma_2 = 1.2$ and 1.4 , it assumes a small value in polycrystal states and increases in the intermediate phase.

Structure Factors of the Densities. – We have visualized the disorder variable D_j and the positions of the large particles in the mixture case, but there should also be some differences in other physical quantities in the ordered and disordered regions in the intermediate phase. To check this possibility, we calculated the structure factor. For the one component case it is defined by $S(k) = \sigma_1^2 \int d\mathbf{r} e^{i\mathbf{k}\cdot\mathbf{r}} \langle \delta\hat{n}(\mathbf{r})\delta\hat{n}(\mathbf{0}) \rangle$, where $\delta\hat{n}(\mathbf{r})$ is the deviation of the density $\hat{n}(\mathbf{r}) = \sum_j \delta(\mathbf{r} - \mathbf{r}_j)$ from the average $n = N/V$. For the mixture case, we define it as [29]

$$S(k) = \sigma_1^2 \int d\mathbf{r} e^{i\mathbf{k}\cdot\mathbf{r}} \langle \delta\hat{n}_{\text{eff}}(\mathbf{r})\delta\hat{n}_{\text{eff}}(\mathbf{0}) \rangle, \quad (7)$$

where $\sigma_1^2 \hat{n}_{\text{eff}}(\mathbf{r}) = \sigma_1^2 \hat{n}_1(\mathbf{r}) + \sigma_2^2 \hat{n}_2(\mathbf{r})$ represents the particle packing fraction with $\hat{n}_\alpha(\mathbf{r}) = \sum_{j \in \alpha} \delta(\mathbf{r} - \mathbf{r}_j)$ being the density of the α -th species. The variable $\hat{n}_{\text{eff}}(\mathbf{r})$ usually exhibits only very small fluctuations for $k \ll 2\pi$ at high densities, while $S(k)$ is sharply peaked with a maximum of order 10 at $k \sim 2\pi$. The wave number k is measured in units of σ_1^{-1} . Figure 4 demonstrates that $S(k)$ is indeed considerably enhanced at long wavelengths in the intermediate phase both in the one and two component cases. This indicates the presence of a small density difference in the two regions, though it is not detectable by eye. To our knowledge, the growth of $S(k)$ at small k has not been discussed in the literature.

Moreover, in the present mixture case, fig. 3 suggests that the structure factor for the composition should be enhanced in the intermediate phase. The composition variable is defined as $\delta\hat{X}(\mathbf{r}) = [(1-c)\hat{n}_2(\mathbf{r}) - c\hat{n}_1(\mathbf{r})]/n$, where

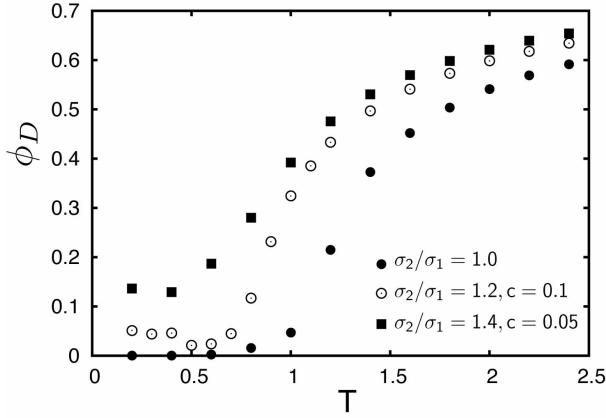


Fig. 4: Fraction ϕ_D of the disordered particles with $D_j > 4$ vs T for (a) $\sigma_1/\sigma_2 = 1$, (b) $\sigma_1/\sigma_2 = 1.2$ and $c = 0.1$, and (c) $\sigma_1/\sigma_2 = 1.4$ and $c = 0.05$.

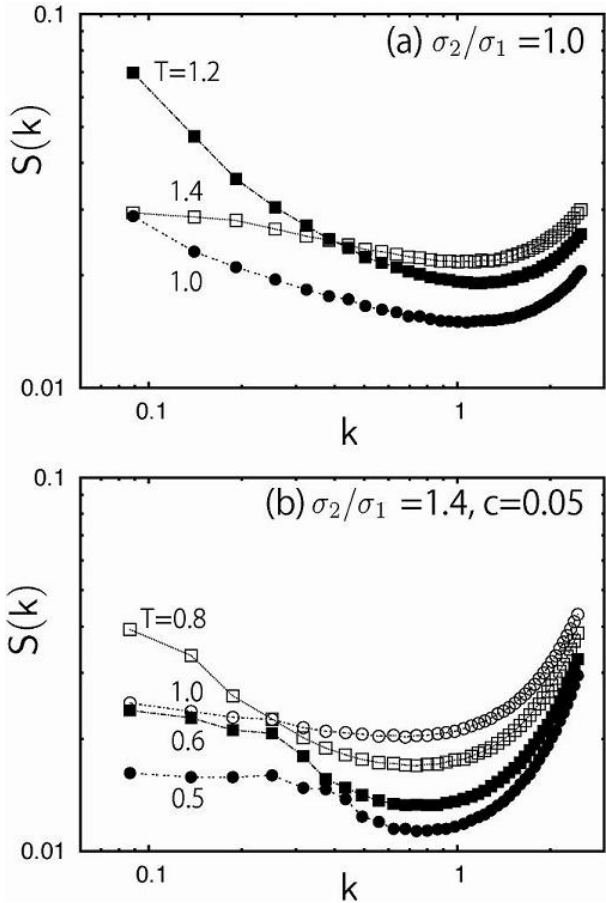


Fig. 5: Long-wavelength structure factor $S(k)$ for $\sigma_2/\sigma_1 = 1$ and $T = 1.0, 1.2$, and 1.4 (top) and for $\sigma_2/\sigma_1 = 1.4, c = 0.05$, and $T = 0.5, 0.6, 0.8$, and 1.0 (bottom), where k is measured in units of σ_1^{-1} . It is enhanced in the intermediate phase. Averages over 5 independent samples were taken for each curve.

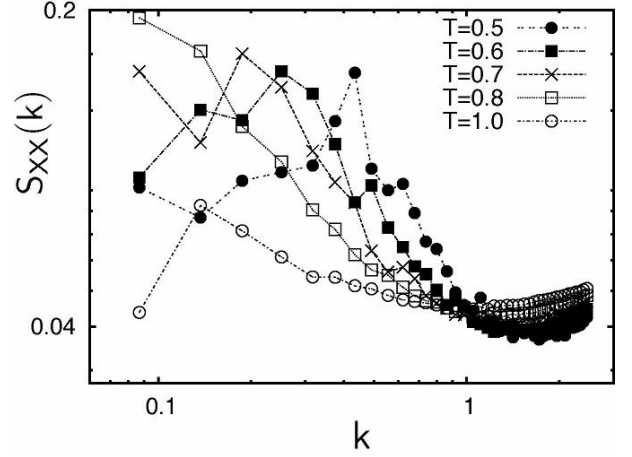


Fig. 6: Composition structure factor $S_{XX}(k)$ in eq. (4) with $\sigma_2/\sigma_1 = 1.4$ and $c = 0.05$ for $k < 1$. It is more enhanced in the intermediate phase. Averages over 5 independent samples were taken for each curve.

$n = N/V$. The structure factor for the composition may be defined as

$$S_{XX}(k) = \sigma_1^{-2} \int d\mathbf{r} e^{i\mathbf{k}\cdot\mathbf{r}} \langle \delta\hat{X}(\mathbf{r}) \delta\hat{X}(\mathbf{0}) \rangle. \quad (8)$$

In fig. 6, this structure factor is dramatically enhanced in the intermediate phase. Since

$$\delta\hat{n}_2 = \frac{c\delta\hat{n}_{\text{eff}} + n\delta\hat{X}}{1 - c + c\sigma_2^2/\sigma_1^2}, \quad (9)$$

we can see $\delta\hat{n}_2 \cong n\delta\hat{X}$ for $c \ll 1$ for $k < 1$. Thus $S_{XX}(k)$ is nearly equal to the structure factor of the large particles $S_{22}(k) = \sigma_1^2 \int d\mathbf{r} e^{i\mathbf{k}\cdot\mathbf{r}} \langle \delta\hat{n}_2(\mathbf{r}) \delta\hat{n}_2(\mathbf{0}) \rangle$ multiplied by $n^2\sigma_1^4$ for $k < 1$. From fig. 3 the enhancement is due to the long range correlation. However, its relatively large size is surprising since $c \ll 1$ here. Indeed, in fig. 6, $S_{XX}(k) \sim 0.2$ at the smallest k ($\sim V^{-1/2}$) for $T = 0.8$, while $S(k)$ reaches only 0.04 in the right panel of fig. 5. The correlation length ξ is of the order of the typical size of the patterns in (b) and (c) of fig. 2. We then estimate

$$S_{XX}(k) \sim c^2(\xi/\sigma_1)^2, \quad (10)$$

for $k\xi < 1$. Here the volume fraction ϕ_D of the disordered region is assumed to be not very small.

Dynamic Heterogeneity. – We now discuss the dynamics around the melting. The heterogeneity time scales in the intermediate phase are very different between the one and two component cases, though the snapshots are rather similar [33]. In one component systems, there is no pinning mechanism of the grain boundary motion. In fact its time scale is of order 10τ in the hexatic state (b) in fig. 1. In binary mixtures with size dispersity, the grain boundaries formed around the large particles are pinned due to the steric effect. In fact, in the time interval $5 \times 10^3 \leq t < 1.5 \times 10^4$, there was no appreciable

large-scale evolution in the patterns in (a) and (b) of fig. 2, while the boundary regions between the ordered and disordered regions locally fluctuated on much shorter time scales in (b). With further increasing T in (c) and (d), the time scale of the patterns decreased abruptly, as can be seen in fig. 7 for (c).

In fig. 7, we display the particles at $t = 8000$ in a quarter of the system with D_j in the one component case at $T = 1.0, 1.2,$ and 1.4 in the mixture case at $T = 0.6, 0.8,$ and 1.0 . We superimpose the particle displacement vectors $\Delta \mathbf{r}_j(t) = \mathbf{r}_j(t + \Delta t) - \mathbf{r}_j(t)$ in a short time interval of $\Delta t = 10$. The particles in the disordered regions can be more frequently mobile than those in the ordered regions. The mobile particles form strings and such strings tend to aggregate, as has been observed in glassy states [29,30]. Thus the intermediate phase is heterogeneous also dynamically (here on a short time scale) [21,32]. In fig. 7, the dynamic heterogeneity obviously originates from the structural heterogeneity around the melting. Such dynamic heterogeneity at the 2D melting has been reported in the previous papers following the particle trajectories [1,11,16]. In glassy states, the dynamic heterogeneity appears on a very long time scale of the structural relaxation time [3,29,30], but we have recently ascribed its origin to the medium-range crystalline order remaining in glass [21,31].

Summary and Comments. – In summary, we have observed continuous melting behavior of one and two component Lennard-Jones systems at fixed volume V . In terms of the disordered variable D_j , emergence of mesoscopic heterogeneity has been evidenced in figs. 1 and 2. The heterogeneity should be treated as an essential characteristic of the intermediate phase, while statistical averages including the pressure p and the correlation function $g_6(r)$ have been calculated in the literature. We note that the visualization in one component systems using the density is elusive with large thermal fluctuations. Nevertheless, we have detected considerable growth of the structure factor $S(k)$ for the density at long wavelengths in fig. 5. Furthermore, in the binary mixture case, the growth of the structure factor $S_{XX}(k)$ for the composition is also enhanced as in fig. 6, because the large particles tend to be trapped in the disordered regions. Marked dynamic heterogeneity in the intermediate phase is demonstrated in fig. 7. The relationship between the structural and dynamic heterogeneities is obvious in this case.

We make further comments. (i) In our simulation, mesoscopic coexistence of the ordered and disordered regions is realized dynamically in an equilibrium state in the intermediate phase. Because the typical heterogeneity size is of order $10\sigma_1$, there are no sharp boundaries between the two regions and the free energy penalty due to the structural inhomogeneity should be very small. Nevertheless, it remains mysterious why no coarsening of the patterns further proceeds beyond the equilibrium characteristic size. It is worth noting that intermediate states are ubiquitous

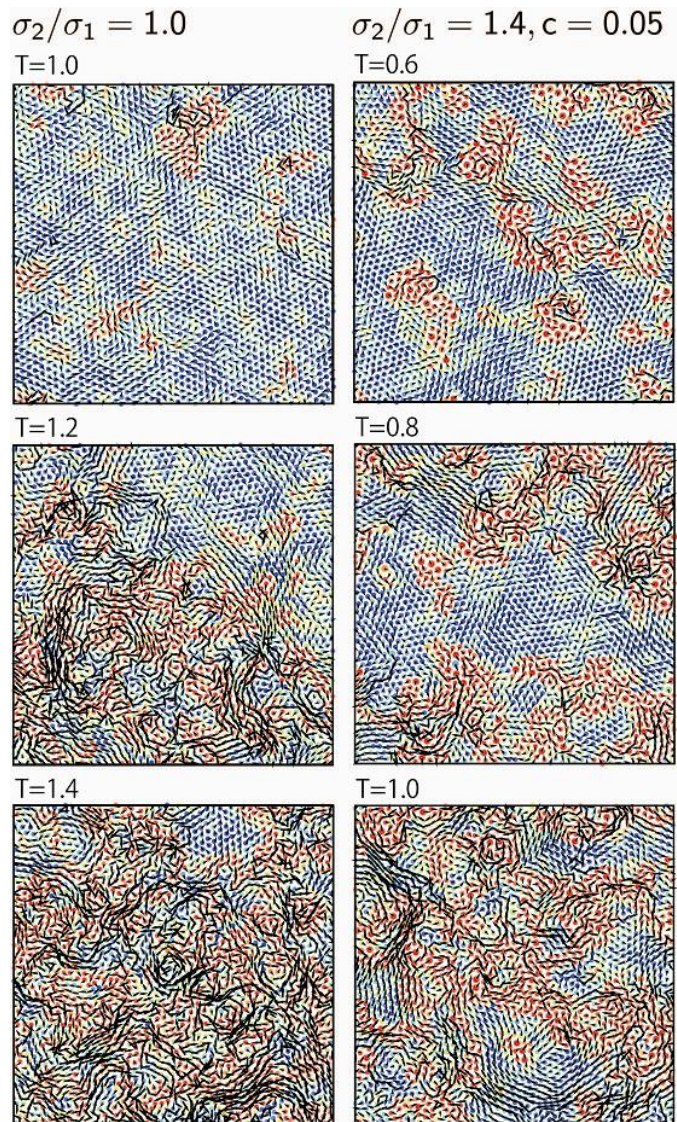


Fig. 7: Disorder variable D_j at $t = 8000$ in a quarter of the system ($0.25V^{1/2} \leq x, y \leq 0.75V^{1/2}$) for the one component case $\sigma_1/\sigma_2 = 1$ with $T = 1.0, 1.2,$ and 1.4 (left) and for the mixture case $\sigma_1/\sigma_2 = 1.4$ with $T = 0.6, 0.8,$ and 1.0 (right). The arrows represent the displacements $\Delta \mathbf{r}_j$ in a subsequent time interval of width $\Delta t = 10$, which are large in the disordered regions than in the ordered regions. The time scales of the particle motions decrease with increasing T . Use of the color is in the same manner as in figs. 1 and 2.

in structural phase transitions in solids [35], where ordered domains are pinned on mesoscopic scales in a disordered matrix in a temperature window. (ii) We also point out that growth (shrinkage) of the disordered regions gives rise to an increase (a decrease) of the pressure p at fixed volume. This is consistent with the large size of the isothermal compressibility in the hexatic phase [3,17–19]. We should perform constant-pressure simulations also to investigate whether or not the intermediate phase depends on the boundary condition. (iii) In the mixture case the

relaxation times are very long even around the melting. Because of this effect, we have not yet completed analysis of $g_6(r)$ in the mixture case. Obviously, we need longer simulations with larger particle numbers. (iv) Shear flow has been applied to glassy systems [29] and to polycrystal systems [32]. It is intriguing how applying shear can affect the intermediate states and the scenario of the melting.

* * *

We thank T. Hamanaka, N. Ito, T. Uneyama, R. Yamamoto, S. Yukawa, and H. Watanabe for valuable discussions. This work was supported in part by Grant-in-Aid for Scientific Research on the Priority Area "Soft Matter Physics" from the MEXT of Japan. H. S. was supported by the Japan Society for Promotion of Science.

REFERENCES

- [1] B.J. Alder and T.E. Wainwright, Phys. Rev. **127**, 359 (1962).
- [2] K.J. Strandburg, Rev. Mod. Phys. **60**, 161 (1988).
- [3] K. Binder and W. Kob, *Glassy Materials and Disordered Solids* (World Scientific, Singapore, 2005).
- [4] F.F. Abraham, Phys. Rev. Lett. **44**, 463 (1980).
- [5] J. Lee and K.J. Strandburg, Phys. Rev. B **46**, 1 (1992).
- [6] H. Weber, D. Marx, and K. Binder, Phys. Rev. B **51**, 14636 (1995).
- [7] B.I. Halperin and D. R. Nelson, Phys. Rev. Lett. **41**, 121 (1978).
- [8] A.P. Young, Phys. Rev. B **19**, 1855 (1979).
- [9] A.H. Marcus and S.A. Rice, Phys. Rev. E **55**, 637 (1997).
- [10] K. Zahn, R. Lenke, and G. Maret, Phys. Rev. Lett. **82**, 2721 (1999).
- [11] K. Zahn and G. Maret, Phys. Rev. Lett. **85**, 3656 (2000).
- [12] R. A. Quinn and J. Goree, Phys. Rev. E **64**, 051404 (2001).
- [13] R.A. Segalman, A. Hexemer, and E.J. Kramer, Phys. Rev. Lett. **91**, 196101 (2003).
- [14] D. E. Angelescu, C.K. Harrison, M. L. Trawick, R. A. Register, and P. M. Chaikin, Phys. Rev. Lett. **95**, 025702 (2005).
- [15] B.J. Lin and L.J. Chen, J. Chem. Phys. **126**, 034706 (2007).
- [16] Y. Han, N.Y. Ha, A.M. Alsayed, and A.G. Yodh, Phys. Rev. E **77**, 041406 (2008).
- [17] A. Jaster, Phys. Rev. E **59**, 2594 (1999).
- [18] S. Sengupta, P. Nielaba, and K. Binder, Phys. Rev. E **61**, 6294 (2000).
- [19] C.H. Mak, Phys. Rev. E **73**, 065104(R) (2006).
- [20] F.L. Sommer, Jr., G.S. Canright, T. Kaplan, K. Chen, M. Motzler, Phys. Rev. Lett. **79**, 3431 (1997).
- [21] T. Hamanaka and A. Onuki, Phys. Rev. E **74**, 011506 (2006); *ibid.* **75**, 041503 (2007).
- [22] S.T. Chui, Phys. Rev. B, **28**, 178 (1983).
- [23] Y. Saito, Phys. Rev. Lett. **48**, 1114 (1982).
- [24] J.A. Zollweg, G.V. Chester, and P.W. Leung, Phys. Rev. B **39**, 9518 (1989).
- [25] M. Hurkey and P. Harrowell, Phys. Rev. E **52**, 1694 (1995).
- [26] M. R. Sadr-Lahijany, P. Ray, and H. E. Stanley, Phys. Rev. Lett. **79**, 3206 (1997).
- [27] W. Vermöhlen and N. Ito, Phys. Rev. E **51**, 4325 (1995).
- [28] H. Watanabe, S. Yukawa, and N. Ito, Phys. Rev. E **71**, 016702 (2005).
- [29] R. Yamamoto and A. Onuki, J. Phys. Soc. Jpn. **66**, 2545 (1997); Phys. Rev. E **58**, 3515 (1998).
- [30] W. Kob, C. Donati, S.J. Plimton, P.H. Poole, and S.C. Glotzer, Phys. Rev. Lett. **79**, 2827 (1997).
- [31] T. Kawasaki, T. Araki, and H. Tanaka, Phys. Rev. Lett. **99**, 215701 (2007).
- [32] T. Hamanaka, H. Shiba, and A. Onuki, Phys. Rev. E **77**, 042501 (2008).
- [33] The pattern in the hexatic state (b) in fig. 1 in the one component case are rather fractal, while those in the binary mixture case are more compact.
- [34] For $\sigma_2/\sigma_1 = 1.2$ the crystalline regions can contain the large particles and the contrast between the two regions become more delicate [21].
- [35] A. Onuki, *Phase Transition Dynamics* (Cambridge University Press, Cambridge, 2002).